

# On empirical methods to predict the rolling period of ships

Rob Grin<sup>1,\*</sup>

## ABSTRACT

*A reliable prediction of the roll period is crucial, as it forms the basis of the calculation of the roll motion and transverse accelerations. Both are extremely important for the comfort and safety of passengers and crew as well as the loads on the cargo and their lashings. At present, some prediction methods are quite unreliable, with sometimes errors in the predicted roll period of 5 to 10 s. This paper describes and compares eight methods. It shows that the four best performing methods have a mean absolute error of less than 1.4 s for the three validation cases evaluated, making them considerably more reliable than some of the other methods used in the industry.*

## KEY WORDS

Rolling period; Radii of inertia; Stability; Seakeeping; Ship motions

## NOMENCLATURE

$A_{\text{lateral}}$	[m <sup>2</sup> ]	Projected side area of ship	H	[m]	Effective depth of ship
$a_{xx}$	[m]	Roll added mass radius of gyration	h	[m]	Height of item
B	[m]	Beam of ship	$h_{\text{tank}}$	[m]	Water height in tank
b	[m]	Width of item	$I_{44}$	[ton·m <sup>2</sup> ]	Roll inertia including added mass
$\beta$	[-]	Roll inertia factor	$I_{\text{fluid}}$	[ton·m <sup>2</sup> ]	Roll inertia of fluid cargo
$b_{\text{tank}}$	[m]	Width of tank	$I_{xx}$	[ton·m <sup>2</sup> ]	Roll inertia
C	[-]	Roll coefficient	k	[-]	Roll factor
$C_b$	[-]	Block coefficient	$k_{\text{spring}}$	[kN/m]	Spring stiffness
$C_u$	[-]	Waterline coefficient of the main deck	$k_{xx}$	[m]	Roll radius of gyration
D	[m]	Depth of ship	$L_{pp}$	[m]	Length between perpendiculars
$\Delta$	[ton]	Displacement	m	[ton]	Mass
$\delta$	[-]	Prefix denoting uncertainty e.g. $\delta GM_t$	MAE	[%]	Mean absolute error
$\delta I_{xx}$	[ton·m <sup>2</sup> ]	Roll added mass inertia	T	[m]	Draft at midship
FSC	[m]	Free surface correction	$T_a, T_f$	[m]	Draft at stern and bow
g	[m·s <sup>-2</sup> ]	Gravitational acceleration (9.81 m/s <sup>2</sup> )	$T_\phi$	[s]	Natural period of roll
$GM_t$	[m]	Transverse metacentric height	VCG	[m]	Vertical centre of gravity

## INTRODUCTION

The rolling period has a large influence on the ship roll motion and accelerations of ships, not only for resonant roll but also for parametric roll. Both are extremely important for the comfort and safety of passengers and crew as well as the loads on the cargo and their lashings. As part of the design verification, seakeeping assessments (either numerical or experimental) are performed. However, when the real roll period is not known, incorrect estimates are made, and the predicted ship

<sup>1</sup> Maritime Research Institute Netherlands (MARIN), The Netherlands

\* r.grin@marin.nl

performance might be misleading. This is also the case when applied to vulnerability criteria within the second generation of intact stability code. At present, many prediction methods are quite unreliable, with errors in the predicted roll period of more than 10% regularly occurring. This paper will give guidelines for the required accuracy that will ensure that the changes in roll behaviour are marginal. Various estimation methods are compared for a range of illustrative ship types. For each of the methods, advantages and disadvantages will be discussed and a practical estimation method will be proposed that can be used both in the ship design phase and in operation.

## ROLL PERIOD AND UNCERTAINTY

The natural frequency ( $\omega_0$ ) of an undamped mass spring system is given by equation 1, where  $k_{spring}$  is the spring stiffness and  $m$  the mass. Assuming that the roll is lightly damped this equation can be used to calculate the roll natural period, see equation 2, in which the roll inertia  $I_{44}$  consists of the total roll inertia including added mass and the spring term  $C_{44}$  is the roll restoring coefficient. This can be rewritten and further simplified to equation 3 as  $\pi/\sqrt{g}$  is around one. In this equation  $k_{xx}$  is the roll radius of inertia,  $a_{xx}$  the roll added mass radius of gyration and  $GM_t$  the transverse stability (see also the chapter on transverse stability if that should be the dry or wet  $GM_t$ ).

$$\omega_0 = \sqrt{\frac{k_{spring}}{m}} \quad [1]$$

$$T_\varphi = 2\pi \sqrt{\frac{I_{44}}{C_{44}}} = 2\pi \sqrt{\frac{I_{xx} + \delta I_{xx}}{g\Delta GM_t}} \quad [2]$$

$$T_\varphi = 2\pi \sqrt{\frac{\Delta k_{xx}^2 + \Delta a_{xx}^2}{g\Delta GM_t}} \approx 2 \sqrt{\frac{k_{xx}^2 + a_{xx}^2}{GM_t}} \quad [3]$$

$$\text{with } k_{xx} = \sqrt{\frac{I_{xx}}{\Delta}} \quad \text{and} \quad a_{xx} = \sqrt{\frac{\delta I_{xx}}{\Delta}} \quad [4]$$

The uncertainty (error) in the rolling period can be estimated if the uncertainties  $\delta k_{xx}$ ,  $\delta a_{xx}$  and  $\delta GM_t$  are known and have a normal distribution (Coleman and Steele, 1999). From equation 3 and after some math, equation 5 gives the total uncertainty in the rolling period. It shows that the  $\delta k_{xx}$  and  $\delta a_{xx}$  make a bigger contribution than the  $\delta GM_t$ , as the uncertainty in  $GM_t$  has a cube root of the  $GM_t$  in the denominator. As the  $k_{xx}$  is typically about twice as large as the  $a_{xx}$  the  $\delta k_{xx}$  is typically bigger than the  $\delta a_{xx}$ . It can therefore be argued that for a small uncertainty in the rolling period ( $\delta T_\varphi$ ), the uncertainty in the  $k_{xx}$  prediction should be reduced as much as possible. This can be illustrated by taking the 77,500 DWT bulk carrier loaded with grain as example (see Appendix A, ship ④). When an uncertainty of 10% is assumed for all 3 input parameters, the roll period is  $16.0 \pm 1.8$  s. If the  $\delta k_{xx}$  is reduced to 5% the uncertainty in the rolling period reduces to 1.3 s, whereas it only reduces to 1.7 s or 1.6 s when the uncertainty of the  $a_{xx}$  or  $GM_t$  reduces to 5%. It is therefore important to get a good prediction of  $k_{xx}$  as it makes the biggest contribution to the rolling period.

$$\delta T_\varphi = \sqrt{\frac{4}{GM_t} (\delta k_{xx}^2 + \delta a_{xx}^2) + \frac{k_{xx}^2 + a_{xx}^2}{\sqrt[3]{GM_t}} \delta GM_t} \quad [5]$$

## EXISTING APPROXIMATION METHODS

Many of the existing methods for monohull vessels use equation 3 as starting point but do not split the roll radius of inertia and the roll added mass. They typically provide the total roll radius inertia as a fraction of the beam of the vessel  $B$  (see equation 6). This factor is called the roll factor  $k$ . Note that in most formulations the factor 2 is contained in the roll factor, causing twice as large a roll factor. Some other formulations use a constant bigger than 2, accounting for the roll added mass. For comparison reasons these variations are not applied in the present work.

$$T_\varphi = 2 \frac{kB}{\sqrt{GM_t}} \quad [6]$$

Some examples for the roll factor are given in Table 1. It is shown that it ranges from 0.33 up to 0.52 and on average 0.42. There seems to be no clear trend; for instance, bulk carriers can be both well below average (BV) or well above (IACS).

**Table 1: List of roll factors**

Source	Ship type	Roll factor k	Remarks
LR, 2022	Container	0.41	
DNV, 2023	All	0.45	Except bulk and ore carriers
	Tanker, ballast	0.40	
ABS, 2019	Container	0.40	
ClassNK, 2023	All	0.40	
BV, 2014	All	0.39	Ore carrier
	Bulk carriers	0.33	
Lewis, 1989	All	0.36	Range: 0.29 – 0.43
IACS, 2012	Bulk carriers	0.40	Homogeneous full load
		0.48	Steel coil
		0.52	Ballast
		0.46	Heavy ballast

Instead of a fixed value, a slightly more complicated estimation of roll factor was proposed by the Shipbuilding Research Association of Japan, JSRA (1982) and IMO (2024). This method is adopted within several IMO documents, for instance the intact stability code (IMO, 2008) and the interim guidelines on second generation intact stability criteria code (IMO, 2020). As shown in equation 7, it increases with the beam over depth ratio ( $B/D$ ) and decreases with ship length. For small vessels this gave satisfactory results, however for large vessels it gives a considerable underestimation of the roll period. For this reason, JSRA made an alternative fit only depending on  $B/D$ -ratio (equation 8). Figure 1 shows the reproduced cross plots of JSRA, with on the x-axis the k-factor recalculated from the measured rolling period of in total 70 vessels and on the y-axis the estimated k-factor according equation 7 and 8. Both fits give fairly equal but considerable scatter, with an  $r^2$  of 0.59 versus 0.43 without ship length dependency.

$$k = 0.373 + 0.023 \frac{B}{D} - 0.043 \frac{L_{wl}}{100} \quad [7]$$

$$k = 0.3437 + 0.024 \frac{B}{D} \quad [8]$$

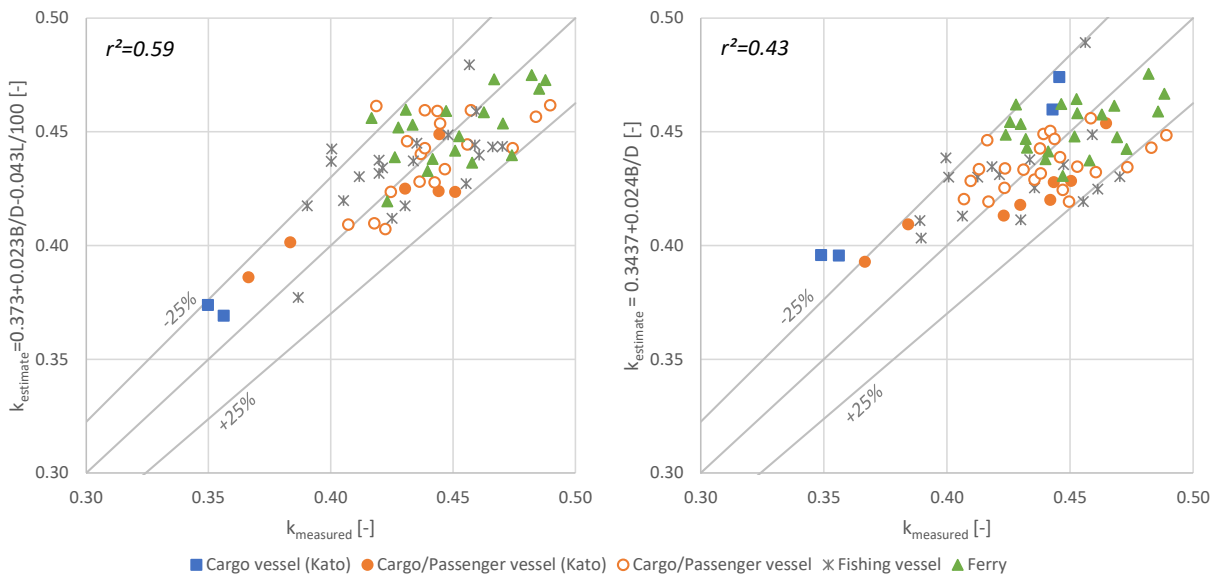


**Figure 1: Reproduced scatter plots according to Shipbuilding Research Association of Japan (1982)**

Much longer ago, Doyere (1927) proposed equation 9 with a ship dependent  $c$ -factor. The formula shows that the rolling period increases with increasing beam and vertical centre of gravity (VCG). According to Doyere, the average  $c$ -factor is 0.29. Doyere provided a table with five naval vessels with multiple loading conditions where  $c$  varied between 0.26 and 0.32.

$$T_{\phi} = c \sqrt{\frac{B^2 + 4VCG^2}{GM_t}} \quad [9]$$

Kato, 1956 proposed equation 10 in which  $T$  is the draft of the vessel,  $C_u$  is the waterline coefficient of the main deck and  $H$  the effective depth (defined as the lateral area divided by the ship length). The factor 0.125 is valid for passenger and cargo vessels. For tankers a value 0.133 was suggested and for navy ships 0.172. It shows that larger  $C_b$  and larger  $H/B$  ratio give a larger roll factor. The  $C_u$  is often close to 1.0 for modern ships; for this reason the middle term is in most cases small compared to the  $C_b C_u$  term and the  $(H/B)^2$  term. It can even become slightly negative.

$$k = \sqrt{0.125 \left( C_b C_u + 1.10 C_u (1 - C_u) \left( \frac{H}{T} - 2.20 \right) + \frac{H^2}{B^2} \right)} \quad [10]$$

Lehmann, 1940, Laurenson, 1949 and Vossers, 1962 assumed that  $k_{xx}$  should be between a solid homogeneous rectangular beam (equation 12) and a rectangular tube with wall thickness of  $0.025B$ . The second is practically identical to a rectangular tube with infinitely thin walls (equation 13). By combining equation 4 and equation 12 and replacing the term  $\sqrt{1/12}$  by coefficient  $c$ , equation 11 is obtained. It results in a  $c$ -value of 0.289 ( $\sqrt{1/12}$ ) and 0.397, respectively. These factors only include the roll mass inertia and not the roll added mass. Laurenson proposed a  $c$  ranging between 0.33 and 0.39, which is very similar to Peach, 1987 suggesting a factor  $c$  of 0.30. Both include the roll added mass. It has to be noted that for ships with heavy cargo concentrated around the centre of gravity (like loaded bulk carriers and tankers),  $c$ -values of less than 0.289 are possible.

Figure 2 shows the resulting curves for Lehmann and Vossers (blue lines), Laurenson (red lines) and the homogeneous rectangular beam and the tube with infinitely thin walls (black lines). Note that for Vossers and Lehmann the line for the empty ship ① is equal to the rectangular tube.

$$kB = c\sqrt{B^2 + D^2} \quad [11]$$

$$\text{Homogeneous rectangular beam: } I_{xx} = \frac{1}{12} m(b^2 + h^2) \quad [12]$$

$$\text{Rectangular tube with infinitely thin walls: } I_{xx} = \frac{1}{12} m(b + h)^2 \quad [13]$$

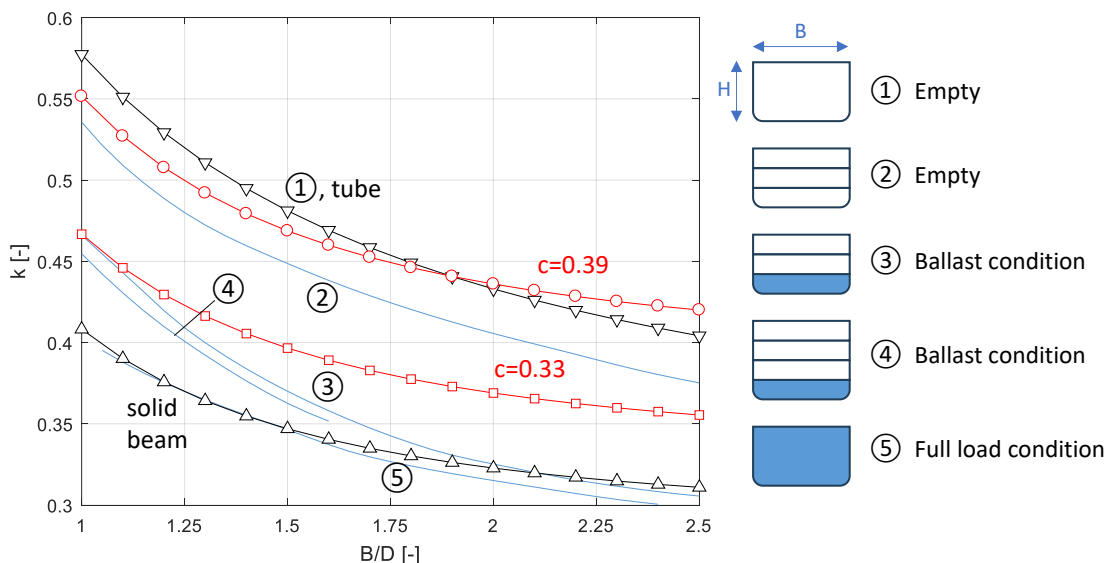


Figure 2:  $c$ -factors as function of B/D ratio

## ROLL RADIUS OF INERTIA

The aforementioned methods estimate the roll factor, which combines the roll radius of inertia and the roll added mass. As there are methods to calculate or estimate the roll added mass (see next section), it would be good to separately calculate or estimate the roll radius of inertia. Preferably, detailed weight calculations are used; however, they are often not available, despite all state of the art CAD tools and software to calculate stability.

Estimation of the  $k_{xx}$  can be done for instance with ITTC, 2017. In equation 14 it is shown that the ITTC formula weights the rectangular tube (first term in the equation) and the solid beam (second term). The last term is a measure for the vertical offset for a half-submerged homogeneous beam (in that case the last term is zero).

$$k_{xx} = \sqrt{\frac{1}{12} \left( 0.4(B + D)^2 + 0.6(B^2 + D^2) - \left( 2T - \frac{D}{2} - VCG \right)^2 \right)} \quad [14]$$

Another estimation method was proposed by Grin et al., 2016, shown in equation 15. This method is based on detailed weight calculations for 9 vessels and in total 16 loading conditions. It also consists of 3 terms. The first term is solid beam with factor  $\beta$  being ship type and loading condition dependent (and 12 for a solid beam, see also equation 12). The second term is accounting for the offset between the real VCG and the VCG for a solid beam ( $H/2$ ). The last term gives a correction in case of fluid cargo. In this case part of the roll inertia of the fluid should be subtracted from  $k_{xx}$ . This is done by the  $c_{fluid}$  factor, which varies between 1 for solid cargo and 0 for fluid cargo in a cylindrical tank (Grin et al, 2016). The suggested  $\beta$ -factors are 9.8 for ships in (near) ballast condition, 11 for ships in loaded condition with a more or less homogeneous mass distribution and relatively high stowage factors and 14.7 for ships carrying cargos with low stowage factor or a large portion of the mass close to centre of gravity.

$$k_{xx} = \sqrt{\frac{B^2 + H^2}{\beta} + \left( \frac{H}{2} - VCG \right)^2 + (c_{fluid} - 1) \frac{I_{fluid}}{\Delta}} \quad [15]$$

## ROLL ADDED MASS

It is recommended to calculate the roll added mass  $a_{xx}$  by means of potential flow strip-theory or panel codes. This gives the most reliable estimate accounting for the hull shape, speed of the vessel and roll period. Note that the roll added mass is also dependent on water depth and presence of side walls (e.g. the quay). In the case of restricted water, the  $a_{xx}$  increases and thereby the rolling period.

In the case of deep water, a first rough estimate can be made using equation 16. This is based on the recalculated  $a_{xx}$  from MARIN model tests of 228 different monohull vessels, varying from small patrol boats to large tankers and container vessels. This estimate assumes that the  $a_{xx}/B$  increases linearly with the  $B/T$  ratio. Figure 3 shows a cross plot of the measured and predicted roll added mass. It shows that correlation is fair, with an  $r^2$  of 0.46.

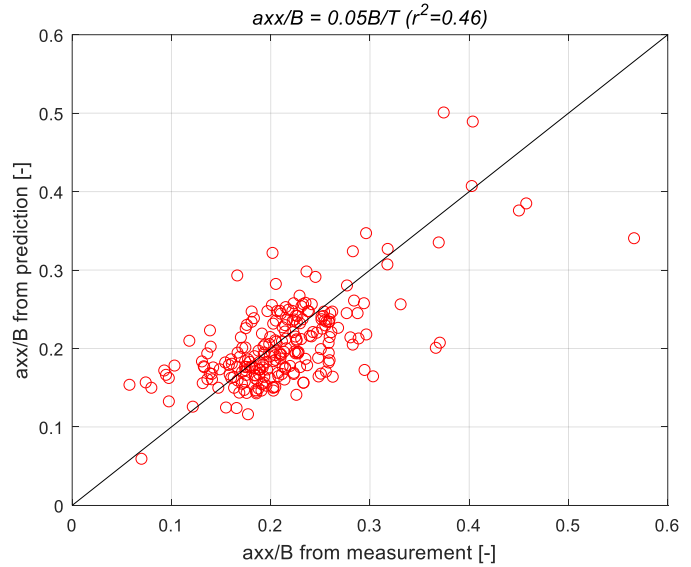


Figure 3: Predicted against measured roll added mass

$$a_{xx} = 0.05 \frac{B^2}{T} \quad [16]$$

## TRANSVERSE STABILITY

The transverse stability is in the denominator of the rolling period equation: the higher the transverse stability ( $GM_t$ ) the lower the rolling period of the vessel (a stiff ship). In most publications it is not clearly stated if the dry  $GM_t$  or the wet  $GM_t$  (including the free surface correction, FSC) should be taken. In IMO, 2020 (SGISC) it is recommended to use the dry  $GM_t$  for excessive accelerations and for the other modes the wet  $GM_t$ . This is considered a conservative estimate by IMO.

Using the wet  $GM_t$  assumes that the fluid in the tanks is always in phase with the roll motion and consequently always at the lee side. For many tank geometries this is indeed true. With equation 17 the natural period of a rectangular tank can be predicted. This further simplifies to equation 18 in shallow water. In this equation  $b_{tank}$  is the width of the tank and  $h_{tank}$  the water level.

$$T_{tank} = \frac{2\pi}{\sqrt{\frac{\pi g}{b_{tank}} \tanh\left(\frac{\pi h_{tank}}{b_{tank}}\right)}} \quad [17]$$

$$T_{tank} = \frac{2b_{tank}}{\sqrt{gh_{tank}}} \quad [18]$$

For example, the natural period is only 1.6 s for a side tank of 2.0 m wide and 7.5 m height and 20% filled with water. Assuming a rectangular double bottom tank with a width of 12.5 m, a height of 2.0 m and also 20% full, this increases to 12.6 s. However, that assumes that there are no obstructions in the tank. In reality, a double bottom tank has many obstructions like longitudinal frames and girders. In Figure 4 an example is shown of the typical double bottom construction of a large container ship. These ships have a girder for each stack of containers, leading to a girder spacing of around 2.5 m. These girders have typically only a few manholes, for instance every 3.5 m one manhole of 700x500 mm and only a few small discharge holes at the bottom of the girders. In the case of a static heel angle the water (or fuel) eventually flows to the lee side. This is why the free surface correction of a double bottom tank is significantly larger than for a side tank. However, in the case of a rolling motion of say 20 to 30 s, the water does not have sufficient time to flow to the lee side and will move mostly in between two girders, and at low water levels maybe even in between two longitudinal frames. It is therefore not realistic to account for the full FSC of these double bottom tanks for the calculation of the roll period. In the previous example of the 12.5 m wide double bottom tank the FSC decreases by a factor 25 if the water moves between girders. In practice this means that for many ships the FSC can be disregarded and the dry  $GM_t$  can be taken in the calculation of the rolling period. However, caution should be taken in the case of for instance large fluid cargo tanks, LNG fuel tanks and other tanks with only few internal obstructions. For these cases the FSC should be included in the calculation of the rolling period. A special case are anti-rolling tanks; these tanks are designed to reduce the roll motion and therefore the water is moving in counterphase of roll motion. For this reason, the FSC of these tanks should be disregarded.

Note that the  $GM_t$  could also be speed dependent. When ships with a flat transom sail at forward speed, the steady wave pattern, trim and sinkage typically increase the waterline area at the stern. This increases the  $BM$  and thereby the  $GM_t$ . As a result, the roll period could decrease somewhat at forward speed.

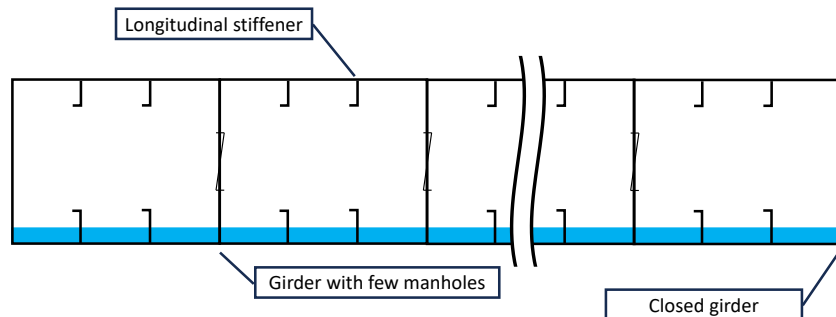


Figure 4: Typical cross section of double bottom tank of a large container ship

## VALIDATION

Two statistical quantities are used for the three validation cases mentioned below: the well-known correlation coefficient ( $r^2$ ) and the mean absolute error (MAE). The first one is a good measure for the scatter but does not show bias, whereas the second one also accounts for bias. Cross plots are presented in which the measured or calculated values are shown on the x-

axis and the predicted values on the  $y$ -axis. With a perfect correlation (an  $r^2$  of 1 and an MAE of 0) all points will be on the diagonal.

**Case 1, detailed weight calculations**

For the first validation case, detailed weight calculations were done for 9 ships and 16 loading conditions (Grin et al., 2015 and Grin et al., 2016). A variety of ship types were used: 2 general cargo vessels, 2 tankers (LNG and LPG), 2 bulk carriers, a container vessel, a cruise ship and a frigate. The main particulars, stability data and roll coefficients are given in Appendix A. The previous publications focused on the detailed weight calculation and the prediction of the roll, pitch and yaw radius of gyration. For this work, strip-theory calculations were done to predict the roll added mass  $a_{xx}$  and on the basis of the given dry  $GM_t$  and the  $k_{xx}$  from the weight calculations, the roll period was calculated.

The cross plots in Figure 5 shows the eight different prediction methods. It is shown that most methods give a fair to good prediction. Even a straightforward method like the roll coefficient method with a fixed value of 0.40 has an  $r^2$  of 0.96 and an MAE of 2.0 s. JSRA (as used by IS2008 and SGICS), Kato and ITTC and are the methods that have the smallest  $r^2$  and highest MAE. On the other hand, the JSRA without the ship length in the empiric formula performs quite well (3<sup>rd</sup> place) with an  $r^2$  of 0.98 and an MAE of 1.4 s. The roll coefficient method (with  $k=0.40$ ), Doyere (with  $c=0.34$ ) and the beam method (with  $c=0.36$ ) fall in the middle. Grin has the best performance, with an  $r^2$  of 0.998 and an MAE of only 0.7 s. It has to be noted that this is logical as the method is based on these ships.

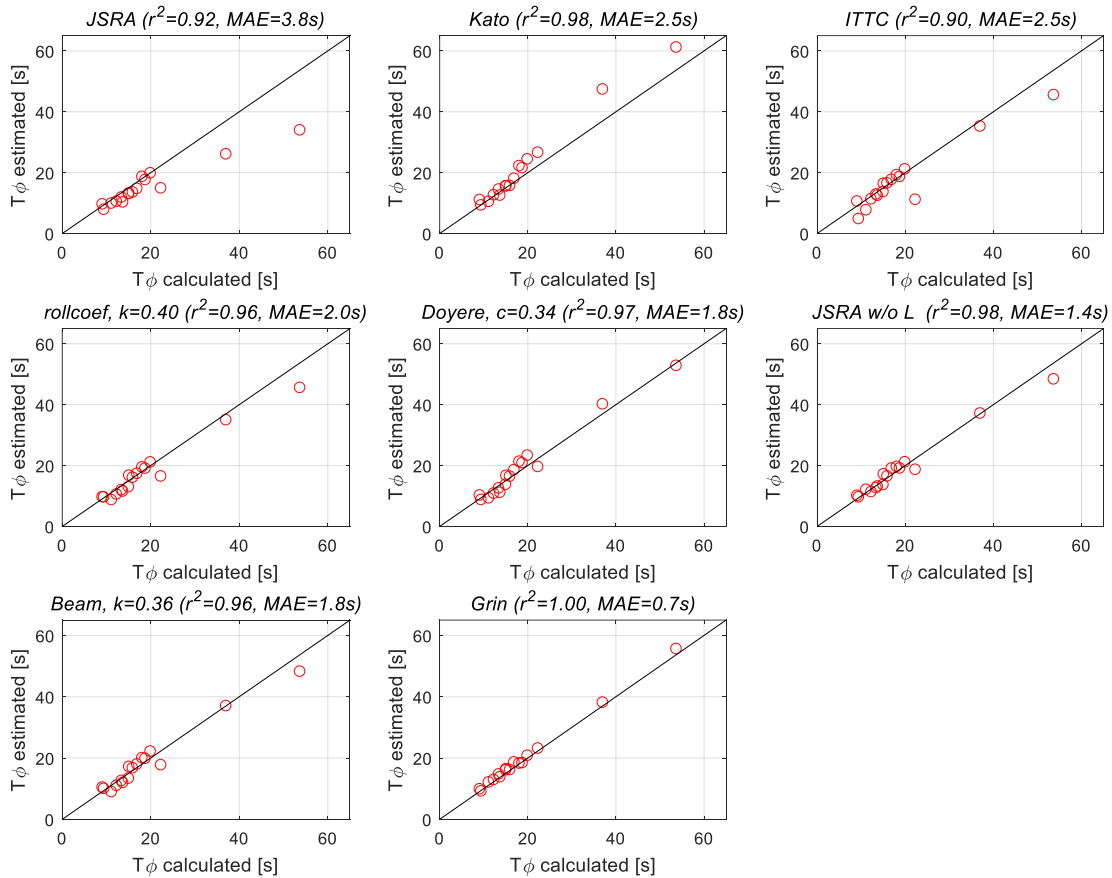


**Figure 5: Cross plots of calculated and estimated rolling period of 9 vessels (16 loading conditions)**

### Case 2, full scale measurement data on a 9200 TEU container vessel

Full scale measurements on a 9200 TEU container vessel were re-analysed within the TopTier joint industry project. This project aims at a significant reduction of containers lost at sea (Koning et al, 2022). A proper estimation of the roll period is very important as it is used in the lashing software to determine if lashing loads are within limits as well as for determining the risk of large roll motions during the voyage. The main dimensions of the vessel are given in Table 2 and Figure 6 shows the side view for one of the voyages including the calculation of the effective depth  $H$  (total lateral area divided by  $L_{pp}$ ).

The measurements were done for a long period of time and for part of this period also the loading conditions for each voyage were stored. In total 114 voyages contained both measurements as well as the loading condition. As shown in Table 2, the variation in loading conditions is large, ranging from (near) ballast conditions to full load condition at almost scantling draft. Also, the GM range was large, from relatively low stability of 1.2 m up to 13.2 m in very light load coastal voyages in Asia. Note that the effective depth is dependent on the arrangement of deck containers and is variable as well.

**Table 2: Main dimensions of the 9200 TEU container vessel**

		min	max
$L_{pp}$	[m]	333.0	
B	[m]	42.8	
D	[m]	27.3	
H	[m]	30.2	49.6
Ta	[m]	7.3	14.8
Tf	[m]	4.9	14.7
$\Delta$	[ton]	47,000	143,000
VCG	[m]	13.3	19.4
GM	[m]	1.2	13.2
FSC	[m]	0.1	1.2
$T_{\phi}$	[s]	11	34.5
$\beta$	[-]	14.7	
Cu	[-]	0.89	

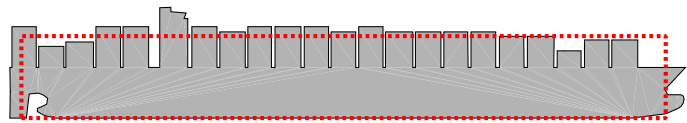


**Figure 6: Side view of the 9200 TEU container vessel**

From all the measurements only the roll motion is used. The sample rate was 20 Hz and data was stored in 1-hour datafiles. The roll period was obtained by a spectral analysis (Welch method) of these 1-hour measurements. A small frequency step of 0.002 rad/s was used to get enough resolution. The drawback is that the spectrum is quite spiky. The peak frequency of the spectrum was stored and if the same peak frequency is measured 10 times, it is considered to be the roll natural period. This procedure is needed as a ship is not necessarily rolling at its natural roll period: this could be easily 5% longer or shorter. This is clearly illustrated in Figure 7. The upper plot shows one 1-hour timestep of the roll motion within one of the voyages. The accompanying roll spectrum is shown in the lower left plot with the largest peak at 0.242 rad/s, resulting in a roll period of 26.0 s in that timestep. After 52 timesteps, the same roll period was found 10 times, being 26.2 s. The histogram shows all 52 roll periods found; they show a considerable spread, from 20.9 s to 32.1 s. It is probably possible to find a more efficient procedure to accurately measure the roll period, but these results illustrate that simply timing 10 roll oscillations is not sufficient for an accurate assessment.

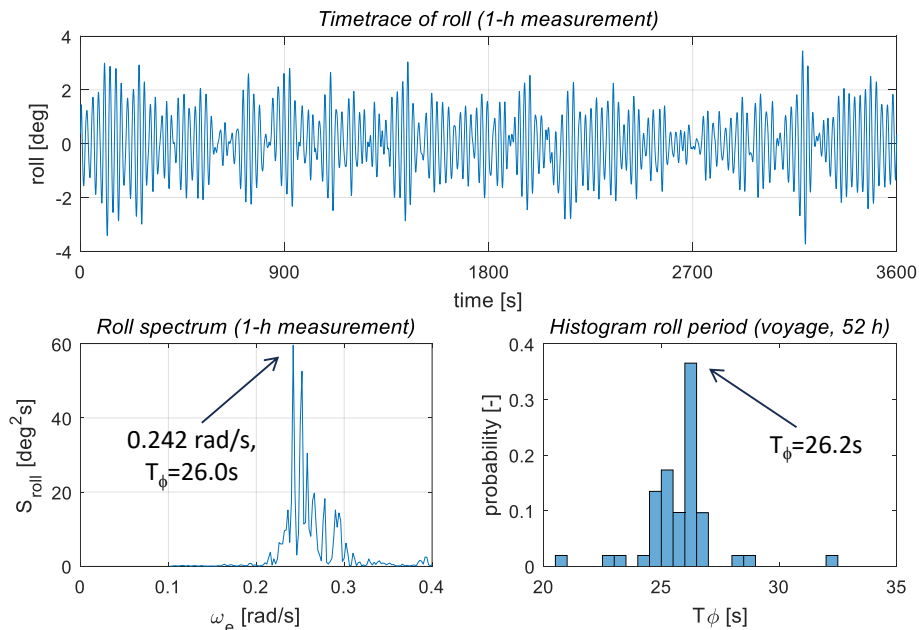


**Figure 7: Example of 1-h time trace, roll spectrum and resulting roll period for the complete voyage**

Similar to the previous case, cross plots are made with the measured roll period against the estimated roll period, see Figure 8. The score is more or less the same, with JSRA and Kato being the worst. The ITTC and the roll coefficient method are in the middle. The top 4 consists of Doyere, JSRA without the length, Grin and the beam method. All 4 methods perform equally well with an MAE of around 0.9 s. Note that the scatter in these plots comes not only from an imperfect fit, but also from uncertainty in  $GM_i$ , as the actual weight and position of the stowed containers might be different from the provided one.

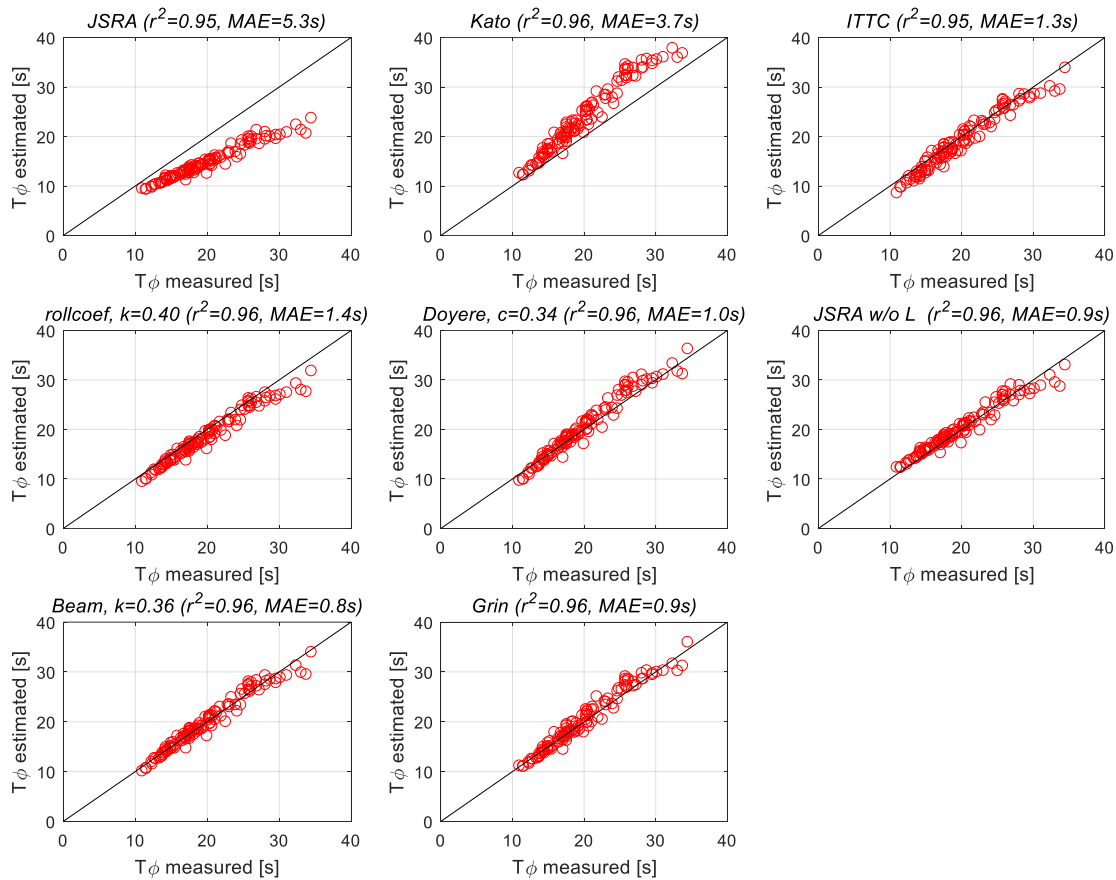


**Figure 8: Cross plots of measured and estimated roll period of 114 voyages of a 9300 TEU container vessel**

### Case 3, full scale measurement data of a 14,000 TEU container vessel

Within the Toptier joint industry project, full scale measurements are ongoing on 3 large container vessels. For the 14,000 TEU vessel part of the measurements are already analysed, resulting in the roll period for 45 voyages. Table 3 shows the main particulars and loading conditions of the vessel. In this case the stow positions of the deck containers was not available. Consequently, the effective depth ( $D$ ) was not calculated per voyage, but an average was taken assuming an average of five high cube containers stowed on deck. As shown in the previous benchmark case the effective depth could vary considerably and this affects to some extent the results of Kato and Grin as both use the effective depth. The roll period is determined using the same analysis procedure as for validation case 2.

Figure 9 shows the resulting cross plots. It is shown that the correlation coefficient is somewhat lower than previous two benchmark cases, mainly caused by a few outliers (whereas the MAE is comparable). After checking these outliers, no reason was found to disregard these voyages. The prediction methods give again similar results, with JSRA and Kato having the largest MAE, ITTC, JSRA without length and the roll coefficient method ending in the middle and Doyere, Grin and the beam method as 3 best performing methods.

**Table 3: Main dimensions of the 14,000 TEU container vessel**

		min	max
Lpp	[m]	340.5	
B	[m]	53.5	
D	[m]	29.9	
H	[m]	47.9	
Ta	[m]	10.8	16.5
Tf	[m]	9.4	16.3
$\Delta$	[ton]	119,000	215,000
VCG	[m]	16.5	23
GM	[m]	2.3	10.4
FSC	[m]	0.2	1.0
$T_\phi$	[s]	14.8	37.9
$\beta$	[-]	14.7	
Cu	[-]	0.96	

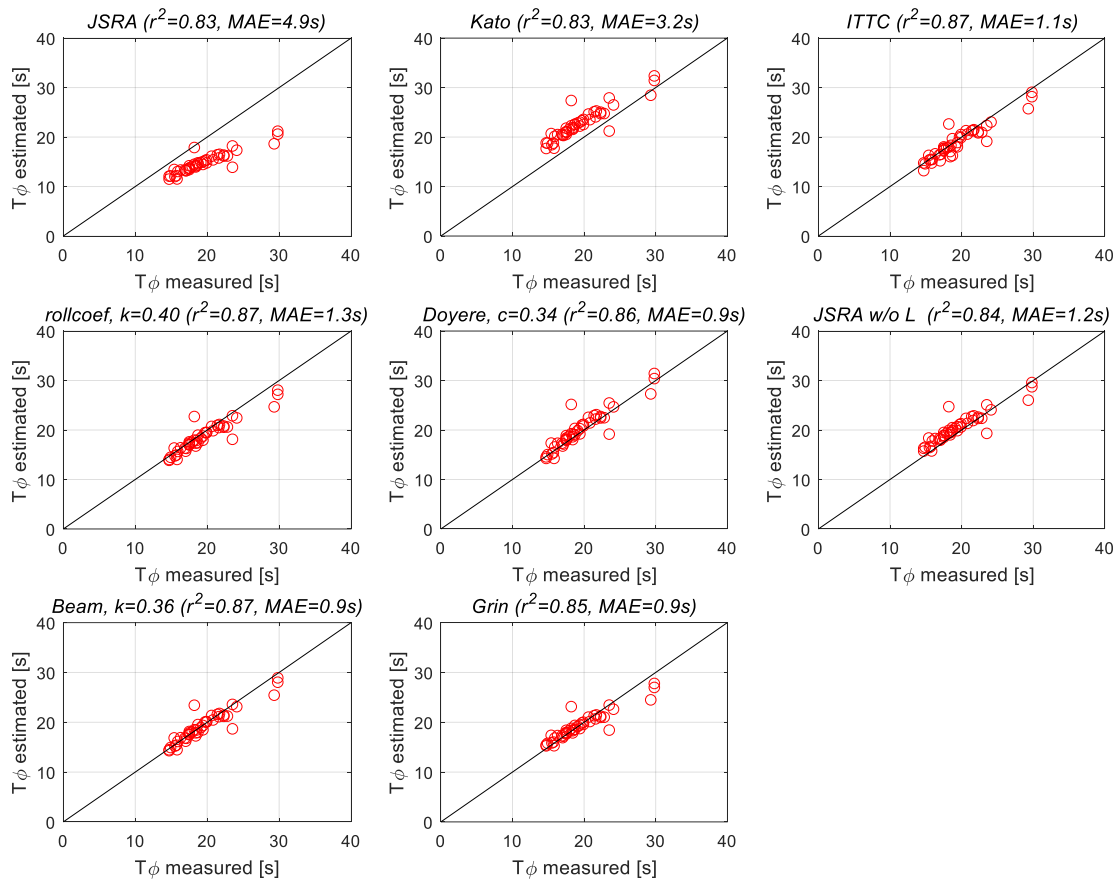


**Figure 9: Cross plots of measured and estimated roll period of 45 voyages of a 14,000 TEU container vessel**

## CONCLUSIONS

A reliable prediction of the roll period is crucial, as it forms the basis of the calculation of the roll motion and transverse accelerations. If the roll period and underlying parameters  $k_{xx}$ ,  $a_{xx}$  and  $GM_t$  are wrong all subsequent calculations are wrong as well. This could have large consequences and might even affect safety when passenger, crew and cargo are exposed to large, unexpected roll motion e.g. due to parametric roll. Within this paper eight methods are evaluated and compared. Based on the present work, the following conclusions can be drawn:

- The uncertainty in roll period comes in large part from the uncertainty in  $k_{xx}$ . The uncertainty in  $a_{xx}$  and  $GM_t$  have roughly equal contribution. In order to reduce the uncertainty in roll period it is best to reduce the uncertainty in  $k_{xx}$ . The difficulty is that  $k_{xx}$  is not as readily available as for instance the  $GM_t$ .
- The  $a_{xx}$  can easily and reliably be calculated with any frequency domain seakeeping code. The  $a_{xx}$  is dependent on hull shape, roll period and water depth. In shallow water the  $a_{xx}$  increases and thereby the roll period. For this reason, onboard measurement of the roll period should take place in deep water. As the  $a_{xx}$  dependency is not very sensitive to loading condition, a fairly small  $a_{xx}$  database with as variables draft and  $GM_t$  would be sufficient and intermediate values can be interpolated from this database. If direct calculation or interpolation from a database is not possible, a rough estimate can be made with equation 16.
- For the prediction of the roll period, the dry  $GM_t$  (without FSC) is typically the best choice. This is because for many ships the FSC mainly originates from the double bottom tanks in which the water ballast or fuel cannot move freely when exposed to rolling because of the internal structure. Also, for anti-rolling tanks the FSC should not be included. The remaining tanks typically have a small FSC which can be included in the rolling period calculation, but if disregarded the error is fairly small. Only in the case of wide tanks without a lot of internal structure like e.g. cargo tanks and LNG fuel tanks, should the FSC be accounted for.
- Eight roll period prediction methods were evaluated. All of them essentially predict the  $k_{xx}$  and except two (ITTC and Grin), all of them include the  $a_{xx}$ . These methods have been compared to three validation cases: 1) detailed weight calculations and strip-theory calculations of 9 different ships with 16 loading conditions in total; 2) full-scale

measurements on a 9200 TEU container vessel consisting of 114 voyages and 3) full-scale measurements on a 14,000 TEU container vessel consisting of 45 voyages.

- Based on these 3 cases it is shown that JSRA (as used in IS2008 and SGICS) and Kato have relatively large errors, with a MAE of 2.5 s up to 5.3 s. All other methods give a fair to good estimate with a MAE of 0.7 s to 2.5 s. The four best performing methods are listed in the table below.

**Table 4: Best performing methods to predict roll period**

Method	$r^2$ , case			MAE [s], case			Pro (+) / cons (-)
	1	2	3	1	2	3	
Doyere, c=0.34	0.97	0.96	0.86	1.4	0.9	0.9	Only B and VCG needed (+), physics based (+), added mass in c-factor (-)
JSRA w/o L	0.98	0.96	0.84	1.4	0.9	1.2	Only B and D needed (+), not based on physics (-), added mass in c-factor (-)
Beam, k=0.36	0.96	0.96	0.87	1.2	0.8	0.9	Only B and D needed (+), physics based (+), added mass in k-factor (-)
Grin	1.00*	0.96	0.85	0.7*	0.9	0.9	Require effective depth H (-), physics based (+), added mass separated (+)

\* It has to be noted that the first validation case is also used within the development of Grin, it is therefore logical that it performs best there.

## FURTHER WORK

Ship stability software has potentially the capability and information (weight, position and geometry of all deadweight mass) to accurately calculate the  $k_{xx}$ . It only requires the radii of inertia of the light ship. This would make estimation methods obsolete; only roll added mass needs to be calculated or predicted.

It is advised to do onboard measurement of the rolling period. This can be used for onboard advice to reduce the risk of large roll motions but also to tune roll factors for the specific ship, and if needed, loading conditions. It is however not straightforward to accurately derive the rolling period from measurements. Guidelines on how to do this should be developed.

The three validation cases showed almost the same four best performing roll period predictors. Within TopTier full scale measurement campaigns on another 2 large containers vessels are ongoing. These will be used to further validate these methods for container vessels. It is recommended to do some further validation work for other ship types as well. After validation, it is suggested to update the roll period formulas in IMO, ITTC and Class to (one of) these four methods.

## ACKNOWLEDGEMENTS

The author would like to acknowledge the participants of the TopTier joint industry project who made this research possible. A second acknowledge goes to the Shipbuilding Research Association of Japan who supplied background information on the alternative JSRA fit without length.

## REFERENCES

ABS (2019), “*The Assessment of Parametric Roll Resonance in the Design of Container Carriers*”, Section 2.4 p23

BV (2014), “*Rules for the Classification of Steel Ships*”, Section 3, 2.4.1

ClassNK (2023), “*Guidelines on preventive measures against parametric roll (Edition 1.0)*”, Appendix 2, p12

Coleman, H. W., and Steele, W. G. (1999), “*Experimentation and Uncertainty Analysis for Engineers*”, 2<sup>nd</sup> Edition, USA

Doyere (1927), “*Théorie du navire*”, p334-337

DNV (2023), “*Rules for classification, Ships*”, Part 3, Chapter 4, Section 3 2.1.1, p28

Grin, R. and Fernandez Ruano, S. (2015). “*On the prediction of Radii of Inertia and their Effect on Seakeeping*” 12<sup>th</sup> International Marine Design Conference Vol 3, pp 189-203

Grin, R., Fernandez Ruano, S., Bradbeer, N. and Koelman, H. (2016). “*On the prediction of Radii of Inertia and their Effect on Seakeeping*”, PRADS2016 Copenhagen

- IACS (2012), “*Common structural rules for bulk carriers*”, Chapter 4, Section 2.1.1
- IMO (2008), “*International Code on Intact Stability, 2008*”, ISBN 978-92-801-17202
- IMO (2020), “*Interim Guidelines On The Second Generation Intact Stability Criteria*”, MSC.1-Circ.1627
- IMO (2024), “*Alternative roll period formula to be used for the second generation intact stability criteria*”, MSC 108/INF.7
- Koning, J., Grin, R. and Pauw, W. (2022), “*TopTier, seakeeping and container cargo securing safety*”, 18th International Ship Stability Workshop, Poland
- ITTC (2017), “*Numerical simulation of capsizing behaviour of damaged ships in irregular seas*”, 75-02-07-044 p7
- Laurenson, R. (1949), “*Ship rolling constants*” Marine Engineering and shipping review p49
- Lewis, E. V. (1989), “*Principles of Naval Architecture, 2nd Revision, Volume 3, Motions in Waves and Controllability*”, SNAME
- LR (2022), “*Rules and Regulations for the Classification of Ships*”, Part 3, Section 14 1.7.1, p563
- Kato, H. (1956), “*Approximate Methods of Calculating the Period of Roll of Ships*”, Journal of the ZOSEN KYOKAI (Society Naval Architects of Japan), Vol.89, pp.59-64.
- Shipbuilding Research Association of Japan (1982), No.114R, “*IMCO research to new stability rules*”, RR24 Research Panel Report, p6
- Vossers, G. (1962), “*Behaviour of ships in waves*”, Ships and marine engines, volume II C p240

**APPENDIX A – MAIN DIMENSIONS AND ROLL PERIOD OF REFERENCE SHIPS**

	① 6,000 m3 LPG Carrier Full load Ballast	② 77,500 DWT Bulk Carrier Full load Full load Iron Ore Grain	③ 12,500 DWT general cargo Full load Ballast homog.	④ 8,000 DWT general cargo Full load Ballast homog.	⑤ 183,000 DWT Bulk Carrier Grain Ballast	⑥ 13,000 TEU ContainerShip 87/TEU 127/TEU	⑦ 173,000 m3 LNG Carrier Full load Ballast	⑧ 100,000 GT Cruise Ship Full load
Lpp [m]	107.0	233.7	134.0	120.0	282.9	355.3	291.7	271.2
B [m]	17.6	32.2	18.95	16.6	45.8	48.92	46.44	36.4
D [m]	9.8	18.7	11.0	10.0	25.1	30.3	26.3	23.8
H [m]	17.1	22.0	17.2	15.8	28.9	52.8	35.0	46.4
Ta [m]	7.2	13.9	8.6	7.6	17.4	14.8	11.6	8.0
Tf [m]	6.9	13.3	7.3	6.4	15.5	14.2	11.6	8.0
Δ [ton]	10,100	88,900	17,000	11,500	180,000	184,000	115,700	55,200
VCG [m]	7.2	6.1	7.7	6.9	14.1	22.7	17.7	17.8
GMt [m]	0.5	7.3	0.6	0.4	4.9	0.7	4.6	3.2
FSC [m]	0.06	0.05	0.13	0.02	0.08	0.11	1.01	0.00
k <sub>xx</sub> [m]	5.9	11.3	7.1	5.9	14.8	21.3	15.8	18.1
a <sub>xx</sub> [m]	3.0	6.1	2.5	2.2	7.9	9.09	9.1	8.3
T <sub>φ</sub> [s]	18.1	9.5	18.8	20.0	15.2	53.8	17.0	22.4
I <sub>fluid</sub> [tonm <sup>2</sup> ]	6.76E+04	0	0	0	0	0	8.38E+05	0
β [-]	14.7	14.7	14.7	14.7	14.7	11.0	11.0	11.0
C <sub>v</sub> [-]	0.89	0.93	0.98	0.98	0.93	0.99	0.85	0.92
T <sub>φ</sub> JSRA [s]	18.6	7.8	17.5	19.7	13.1	33.9	14.6	14.8
T <sub>φ</sub> Kato [s]	22.1	9.2	21.5	24.3	15.5	61.1	17.9	26.5
T <sub>φ</sub> Doyere (c=0.34) [s]	21.2	8.7	20.8	23.2	16.6	52.7	18.4	19.5
T <sub>φ</sub> Rollcoef (k=0.4) [s]	19.3	9.5	19.0	21.0	16.6	45.5	17.2	16.4
T <sub>φ</sub> ITTC [s]	19.2	4.7	18.5	21.0	16.3	45.4	17.6	11.1
T <sub>φ</sub> Grin [s]	18.2	9.1	18.3	20.7	16.4	55.5	18.5	23.0
T <sub>φ</sub> JSRA w/o L [s]	19.5	9.5	19.0	21.0	17.1	48.3	19.0	18.6
T <sub>φ</sub> Beam (k=0.36) [s]	18.8	9.9	18.6	20.8	17.1	50.8	17.8	18.6